IEEE Access
Multidisciplinary | Rapid Review | Open Access Journal

Received October 11, 2020, accepted October 25, 2020, date of publication November 3, 2020, date of current version November 17, 2020.

Digital Object Identifier 10.1109/ACCESS.2020.3035534

Control and Stabilization of Centimeter Scale Glow Discharge in Ambient Air Using Pulse-Width Modulation

VLADISLAV GAMALEEV, (Member, IEEE), NIKOLAY BRITUN, AND MASARU HORI, (Member, IEEE)

Center for Low-Temperature Plasma Sciences, Nagoya University, Nagoya 468-8603, Japan

Corresponding author: Vladislav Gamaleev (vlad@plasma.engg.nagoya-u.ac.jp)

This work was supported in part by the JSPS KAKENHI under Grant 19H05462, and in part by the Plasma-Bio Consortium Project under Grant 01221907.

ABSTRACT Re-pulsing glow discharges in atmospheric-pressure air were experimentally investigated using a push–pull generator with pulse-width modulation. Discharges were ignited as a spark-glow discharge sequence and sustained in a glow regime after ignition in a gap of 2 cm and characterized by current and voltage measurements, as well as by optical emission spectroscopy. It was found that at a certain range of parameters, the discharge could be stabilized even in the presence of external airflow. It was demonstrated that the type of discharge and total power dissipated in the plasma volume could be precisely controlled by pulse-width modulation. Additionally, it was confirmed that the rotational temperature varied across a wide range (1640–2440 K) by using pulse-width modulation with gas-flow control, when vibrational temperature was around 4610 ± 770 K. The generation of stable glow discharge in the presence of gas flow with a wide range of parameters that could be precisely controlled by pulse-width modulation looks promising for use in energy-efficient gas conversion.

INDEX TERMS Glow discharge, gliding arc, OES, air plasma, PWM.

I. INTRODUCTION

The rapid development of atmospheric-pressure plasma sources over the last two decades has led to the use of plasma in a large number of applications where samples are not compatible under low-pressure conditions [1]–[5]. Additionally, the development of nonequilibrium (so-called ''cold'') atmospheric-pressure plasma allowed the plasma treatment of biological targets and opened doors for the use of plasma technologies in medicine, agriculture, and even farming [3], [6]–[14]. On the other hand, growing demands in nitric compounds, which are a crucial part of most fertilizers, led to the requirement for the large-scale production of ammonia and nitric oxide, which are commonly used as precursors for the synthesis of more complex molecules [15], [16]. The most common way to produce ammonia and nitric oxide from nitrogen molecules (so called ''nitrogen fixation'') is the Haber–Bosch process. However, the Haber–Bosch process requires high energy consumption and produces a high level of carbon dioxide emissions; therefore, the efficient replacement of the Haber–Bosch process is required, taking into account growing environmental concerns [16]. Nonequilibrium atmospheric-pressure plasma sources are looking promising as a possible replacement of the Haber–Bosch process for nitrogen fixation [15], [16]. There are few works reporting nitrogen fixation using atmospheric-pressure plasma sources with considerably high efficiency that, together with the use of renewable-energy sources (solar- and wind-power plants), can make plasma a ''green'' technology for nitrogen fixation [15], [17]–[21].

According to a recent report, one of the most efficient plasma sources for nitrogen fixation is the ''gliding arc'' reactor [15], [20]. The term ''gliding arc'' was initially suggested based on the visual appearance of the discharge; however, a more detailed study revealed that this type of discharge burns in a glow regime. Therefore, in the present work, we use the more physically correct term ''gliding glow'' discharge instead of the frequently used ''gliding arc'' [22]–[24].

The associate editor coordinating the review of this manuscript and approving it for publication was Qingli Li.

In general, glow discharges are one of the most studied types of plasma; however, most detailed studies were done in low-pressure conditions [25]–[28]. Two main features are required for the possible application of glow discharge in gas conversion: operation at atmospheric pressure and easy scaling. Additionally, air looks promising as a raw material for plasma-based nitric oxide synthesis owing to its low cost; therefore, a scalable atmospheric-pressure ambient-air plasma source is required for sustainable ''green'' nitrogen fixation. There are many works on the generation and diagnostics of glow discharges in various gases at atmospheric pressure using subcentimeter gaps between electrodes, but works are limited on the generation and diagnostics of glow discharges in centimeter-order gaps filled with atmospheric-pressure molecular gases, including air [24], [29]–[34].

Typically, glow discharges in large gaps (greater than 1 cm) in ambient air are initiated using an additional discharge system or as a sequence of spark and glow discharges. For ignition of a spark discharge in atmospheric pressure air using DC or low frequency sinusoidal power supply, approximately 10 kV per centimeter of the discharge gap length (for needle electrodes) or more (up to 30 kV/cm for large spherical electrodes) is necessary, resulting in the use of bulky power supplies even for gaps of a few centimeters [35], [36]. A commonly used approach to scale up glow discharge in air avoiding breakdown in a long gap is the initiation of discharge between electrodes with a smaller gap and subsequent extension of the gap length to the desired value [29], [37]. However, the main drawback of the extension of the discharge gap is the need to use a manipulator and adjust the gap prior to discharge ignition. Atmospheric-pressure glow discharges in molecular gases are easily disturbed and terminated by external airflow, which results in the need to manipulate electrodes during the treatment of large gas volumes. A gliding glow discharge generator is a way to overcome problems with adjusting the discharge gap in the case of discharge termination. A common approach for the generation of gliding glow discharges is using electrodes with extended length of the discharge gap, and gas flow to move glow discharge from the area with the shortest discharge gap to an area with a longer gap [38], [39]. In this case, discharge is initiated in the place with the shortest discharge gap, and elongated during movement towards a long discharge gap to the point where the discharge length exceeds the maximal length that could be sustained by the power supply. At the critical length, discharge is terminated and restarted after termination at the place with the shortest gap. There are two typical electrode geometries used for the generation of gliding glow discharges: planar knife-shaped electrodes [38], [39] and coaxial electrodes with tangential gas flow [40]–[42]. Knife-shaped electrodes are typically used for small-scale reactors when coaxial geometry could be used for the treatment of large gas volumes.

Gliding glow discharges feature high yield and higher energy efficiency for nitrogen fixation compared to other plasma sources [15], [21], [42], [43] and could be scaled for the production of large volumes of NO_x (on the order of L/min) in the case of coaxial electrode geometry [40]–[42]; however, gliding glow plasma sources have several significant drawbacks that are not commonly discussed. First, a certain range of plasma parameters is required for effective gas conversion when plasma parameters in a gliding glow reactor vary in a wide range during the cyclic discharge elongation. Depending on the geometry and characteristics of the power supply, discharge could be initiated as a spark, arc, or in an abnormal glow regime, and with elongation of the discharge, it could change to normal and subnormal glow regimes. In this case, the gas temperature changes from high in the area of discharge initiation (typically above 3000 K), to moderate in the middle of the elongation (typically between 2000 and 3000 K), and to low in the area of maximal elongation (below 2000 K). It was reported that a low-temperature area of gliding glow is desired for effective nitrogen fixation when another part of the plasma in a higher-temperature region is not required due to the loss of energy on excess gas heating [38]. Changing the plasma regime during cyclic elongation between spark, arc, abnormal glow, normal glow and subnormal glow (depending on the setup), when the most efficient is subnormal glow regime (low temperature area), results in gas overheating and ineffective electric power use. Additionally, the presence of plasma with undesired parameters could result in the production of unwanted reactive species, which could limit the application. For example, the production of OH radicals in ambient air glow discharge dramatically increases when the discharge mode is changed from subnormal to normal glow regime [24], and in the case of gliding glow discharge, the production of OH radicals will vary depending on the plasma elongation. Another drawback is the constantly changing plasma impedance that results in problems with load matching and large values of reflected power. In most of the works on nitrogen fixation by gliding glow discharges, electric power dissipated in the plasma was used in the estimation of energy efficiency while the total electric power consumed by the power supply is not commonly discussed. Despite the high efficiency when only power dissipated in the plasma is considered, poor load matching and large power losses during the generation of plasma could be a problem for practical application. On the other hand, the constant change of current and voltage and the restrike of the discharge results in the presence of significant electromagnetic (EMI) noise during operation which might be harmful for surrounding devices and workers.

The perfect solution is the initiation of the discharge in larger gaps at desired parameters, avoiding discharge elongation. A recent work reported glow discharge generation at defined conditions in centimeter-order gaps (up to 2 cm) using a single power supply that did not require any adjustments after the start of the discharge [24]. In the present work, we improved the performance of the previously reported power supply and confirmed the stable operation of plasma with defined parameters in the presence of external airflow without elongation, which looks promising for gas-conversion applications.

II. EXPERIMENTAL SETUP

Re-pulsing glow discharge was generated using a modified version of a generator reported in detail elsewhere [24]. The discharge was ignited between two copper rod electrodes (99.5% Cu, CU-112544, Nilaco, Japan) by supplying high voltage to the upper electrode (anode) when the lower electrode (cathode) was electrically grounded. High voltage was provided using a custom power supply. Pulsed low-voltage sinusoidal signals were generated by a push–pull generator with pulse-width modulation (PWM). The push–pull generator was powered by a regulated direct current power supply unit (DC PSU). The generated pulse-width modulated sinusoidal signal was supplied to the primary winding of a high-voltage transformer. The produced high-voltage signal was rectified using a diode rectifier and stored in a reservoir capacitor to achieve high voltage. In the present work, approximately 1 m of high-voltage wire, a high-voltage probe and the parasite capacitance of other components were used as a reservoir capacitor. The push–pull generator with pulse-width modulation used in the present work was operated normally in the PWM frequency range from 100 Hz to 5 kHz, and the PWM duty cycle was in the range of 5% to 45%.

A schematic layout of the experiment setup is presented in Figure 1.

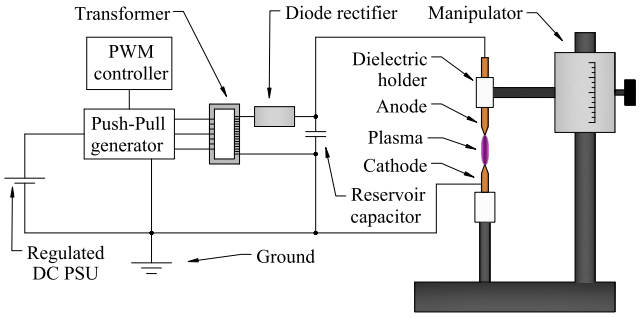

FIGURE 1. Experimental setup.

The gap of 2 cm between the electrodes was adjusted using a manipulator prior to discharge generation and was kept the same during diagnostics.

Current and voltage waveforms were recorded using a high-voltage probe (P6014, Tektronix) and a current monitor (2877, Pearson), and stored in a digital oscilloscope (GDS-3504, Instek).

Optical emission spectra (OES) of the discharge were recorded using a monochromator with 50 cm focal length (Shamrock 500i, Andor; 1200 or 2400 grating) with an ICCD camera (iStar DH734-18U-03, Andor) and a UV transparent lens (UV-Nikkor 105 mm F4.5, Nikon). The relative spectral response of the Monochromator and detector has been measured using a tungsten halogen lamp without performing the absolute (radiometric) calibration. The nonuniform spectral response (Figure S7b, supplementary data) of the spectroscopic system is omitted for the emission spectra given below; however, it was taken into account for the vibrational and rotational temperature calculations. The wavelength calibration was performed using a Hg reference lamp with a precision of approximately 0.03 nm. The time-average plasma photographs were taken using a Nikon D800 digital camera with Nikon 85 mm f/1.8 D lens.

III. RESULTS AND DISCUSSION

A. GENERATION OF PULSE-WIDTH-MODULATED CORONA AND SPARK DISCHARGES

In the case without pulse-width modulation, the signal produced by the push–pull generator was controlled by limiting the voltage and current supplied by the DC PSU to the push–pull generator [24]. In this work, the DC PSU voltage was set to 27 V (resulting in a maximum of 25 kV across the secondary winding after fully charging the reservoir capacitor), and the current on the DC PSU was limited to 5 A (which is above the maximal value supplied during the experiments). The maximal current supplied to the discharge was limited by the leakage inductance of the transformer owing to the weak magnetic coupling between the primary and secondary windings. Since the DC power supply did not limit the discharge current, the electric power delivered to the plasma was defined by the duty cycle set on the PWM controller.

After starting the DC PSU with the preset values of PWM frequency and duty cycle, the reservoir-capacitor charging was started by the generator up to the voltage defined by the duty cycle (alternating process of the charging capacitor during the On stage by the generator, and loss of charge owing to the leakage currents during the Off stage). A typical oscillogram demonstrating the process after starting the generator with the preset parameters is depicted in Figure 1Sa (supplementary data). In our case, it was possible to generate corona discharge, corona with repeating spark discharge, or re-pulsing glow discharge depending on the value of the duty cycle and frequency preset on the PWM controller prior to starting the generator.

In the case of the duty cycle varying in the range of 5% and 10%, the reported generator worked as a high-voltage power supply with a large AC ripple caused by the loss of charge during the Off stage (Figure 1Sb, supplementary data). If voltage supplied by the generator was high enough, corona discharge could be generated. Examples of current and voltage waveforms of corona discharge generated at a frequency of 1 kHz and duty cycle of 10% superimposed with the PWM trigger signal are presented in Figure 2.

The appearance of corona discharge could change from a barely visible point to a diffuse mode filling the entire discharge gap (Figure 2S, supplementary data), similar to diffuse corona discharge reported elsewhere [44]. In the case of corona discharge, the presence of the discharge current resulted in a faster loss of charge during the Off stage (Figure 2b) and large AC ripple (approximately 5 kV) compared to the case when plasma was not observed (approximately 2 kV, Figure 1Sb, supplementary data).

When the duty cycle surpasses 13%, the reservoir capacitor could be charged to approximately 22 kV during the On stage, which was close to the breakdown voltage for

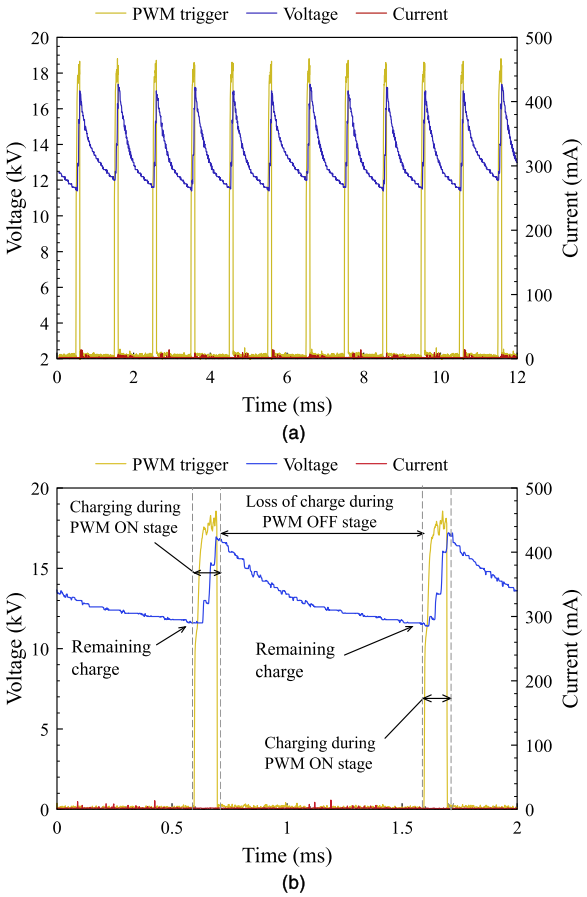

FIGURE 2. Typical current and voltage waveforms of corona discharge superimposed with pulse-width modulation (PWM) trigger signal (a), and enlarged current and voltage waveforms demonstrating PWM effect (b).

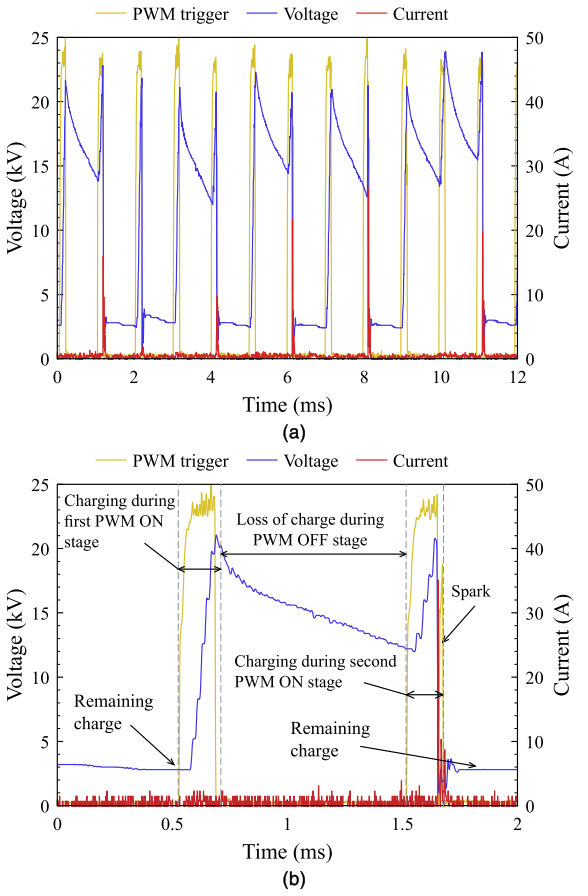

FIGURE 3. Typical current and voltage waveforms of repeating spark discharge superimposed with PWM trigger signal (a), and enlarged current and voltage waveforms demonstrating PWM effect (b).

pin-to-pin electrodes with the 2 cm gap in ambient air. As a result, if the duty cycle increases above 13%, spark discharges occasionally occur if the voltage applied to the electrodes exceeded some threshold value. Examples of the current and voltage waveforms of repeating spark discharges generated at a frequency of 1 kHz and duty cycle of 15% superimposed with the PWM trigger signal are presented in Figure 3, and a picture of the spark discharge is demonstrated in Figure 3S (supplementary data).

Spark discharges can be observed in Figure 3a at approximately 1, 2, 4, 6, 8, and 11 ms. In most cases, two On stages are required for charging the capacitor to the breakdown voltage; however, spark discharge was initiated after one On stage at 2 ms, and another spark discharge was generated after three On stages at 11 ms. Such instability of spark-discharge generation could be explained by the variation of the remaining charge stored in the reservoir capacitor after discharge. As can be observed in Figure 3b, some charge remains in the reservoir capacitor after the spark discharge. If the spark discharge happens during an On stage, it would result in a rapid drop of charge on the reservoir capacitor and termination of the discharge when there is no charge left. However, after discharge termination, the reservoir capacitor would still be charging and accumulating energy until the end of the On stage. The remaining charge left in the capacitor before the start of the subsequent On stage is defined by the duration of the Off stage and the timing of the previous breakdown. The moment of spark-discharge generation has a typical jitter of few tens of μs, resulting in the variation of the charging period after spark discharge.

B. GENERATION OF PULSE-WIDTH-MODULATED GLOW DISCHARGE

If the duty cycle is high enough, a sequence of spark and glow discharge [45]–[47] could happen during an On stage. Moreover, if the frequency set on the PWM controller is high enough for afterglow to remain in the discharge gap during an Off stage, glow discharge could be reignited during the On stages, avoiding the presence of spark for discharge initiation (re-pulsing glow discharge).

The current and voltage waveforms of re-pulsing glow discharge generated at a frequency of 1 kHz and duty cycle of 25% superimposed with the PWM trigger signal are shown in Figure 4.

Glow discharges generated with PWM are highly stable (compared to repeating spark discharges) and appear during each On stage. The enlarged image of the current and voltage waveforms (Figure 4a) shows that discharge ignition is

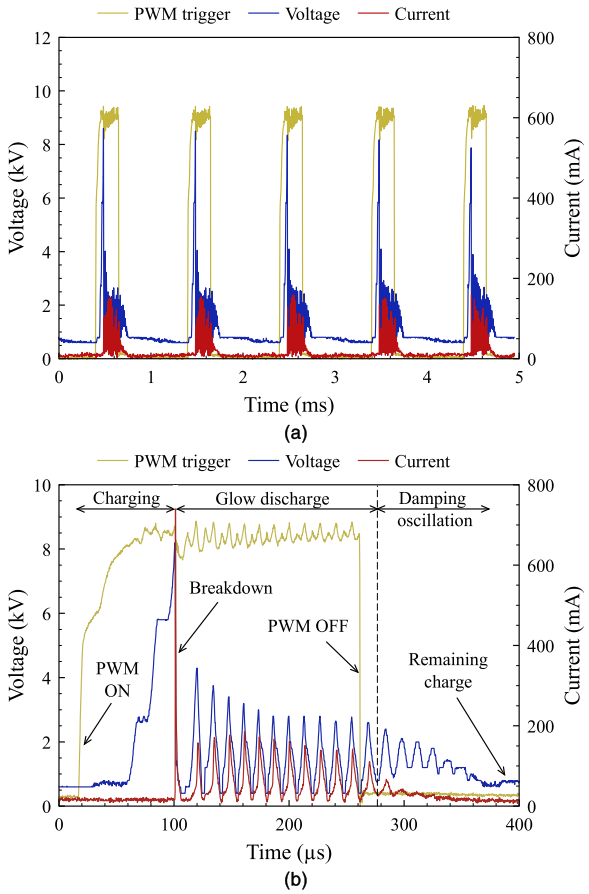

FIGURE 4. Typical current and voltage waveforms of re-pulsing glow discharge superimposed with PWM trigger signal (a), and enlarged current and voltage waveforms of re-pulsing glow discharge during a single PWM On stage (b).

similar to repeating spark discharge. After the PWM trigger, it takes some time to start the push–pull generator and begin charging the reservoir capacitor. When the reservoir capacitor is charged to the threshold value, the breakdown of the discharge gap followed by re-pulsing glow discharge happens. Re-pulsing glow discharge within the PWM On stage appears to be the same as for the case without PWM, reported elsewhere [24]. As a result, the first plasma pulse within a single PWM cycle always possesses a high current, with a peak value depending on the Off stage duration. A decrease of the Off stage duration leads to the presence of plasma afterglow at the moment of breakdown, resulting in a decrease of the breakdown voltage. Since the peak current in the first pulse is defined by the charge of the reservoir capacitor, a decrease in the breakdown voltage should lead to a decrease of this charge at the moment of breakdown, also decreasing the peak current. The first impulse after the breakdown appears to be similar to a spark discharge; however, a more detailed examination suggests that discharge during the first impulse burns in a glow regime (normal or abnormal considering the peak values of the discharge current of few hundreds of mA). The typical duration of spark discharge at a low duty cycle is below 50 ns (see Figure 4Sa, supplementary data), in the case when the re-pulsing glow discharge duration of the first impulse is on the order of microseconds (see Figure 4Sb supplementary data), which is too large for spark discharge. Additionally, the peak current in the case of spark discharge is typically on the order of a few tens of A, whereas in the case of re-pulsing glow discharge, it is typically below 1 A, which is not sufficient for a spark discharge. Taking into account the duration of the impulse and the values of the current, it could be concluded that during the first impulse, plasma is reignited in a glow regime in the afterglow of the discharge, in a similar way as reported elsewhere for the case of gliding glow discharge [48].

Typically, the second plasma pulse (which corresponds to the second positive half cycle of the rectified sinusoidal signal after the first impulse) has a low current owing to the small value of the remaining charge on the reservoir capacitor after the first intense impulse. The following pulses are all defined by the parameters of the sinusoidal signal: rises during a positive half cycle and decays during a negative half cycle (reservoir capacitor is not charged during the negative half cycle owing to the diode rectifier); the peak current and voltage are dependent on the amplitude of the sinusoidal signal. Those plasma impulses are generated in the same way as reported elsewhere, and could be characterized as a glow discharge [24]. Therefore, the plasma discharge is terminated when the voltage drops below the cathode fall value required to sustain the discharge, resulting in the same value of the remaining charge stored in the reservoir capacitor after each impulse. The same value of the remaining charge after each impulse result in a high impulse stability, starting from the third impulse during a PWM On stage compared to the first two impulses.

The push–pull generator does not switch off immediately at the end of the PWM On stage triggering signal, resulting in one plasma impulse after the end of the PWM On stage trigger, followed by damping oscillation caused by energy stored in the capacitors and inductors in the push–pull generator; no plasma was observed during the damping oscillation. After the damping oscillation, there are insignificant leakage currents that cause a small loss of charge during the PWM Off stage, and the value of the remaining charge prior to the next PWM On stage is defined by the duration of the PWM Off stage, as was discussed above.

If the discharge is generated with the values of the duty cycle and frequency of the PWM controller set prior to turning on the generator, large values of the duty cycle (above 18% depending on the frequency) are required for the stable generation of re-pulsing glow discharge. However, after discharge initiation and stabilization, the value of the duty cycle could be reduced while keeping glow discharge stable.

Figure 5 summarizes the duty-cycle values required for the direct ignition of stable glow discharge and the minimal duty-cycle values required to sustain glow discharge (obtained by the reduction of the duty cycle after ignition) at various frequencies.

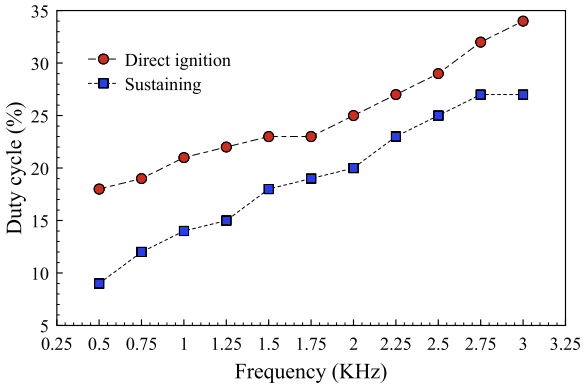

FIGURE 5. Minimal values of PWM duty cycle required for direct ignition and sustaining re-pulsing glow discharge as a function of PWM frequency.

The observed linear trend implies that minimal (threshold) On stage duration is always required for stable discharge ignition. If the duration of the On stage is not long enough to charge the reservoir capacitor to the breakdown voltage and lead to at least one impulse of glow discharge, only spark discharge will occur.

C. EFFECT OF PULSE-WIDTH MODULATION ON THE ELECTRIC PROPERTIES OF GLOW DISCHARGE

Re-pulsing glow discharge could be generated in a wide range of duty cycles and frequencies using the reported device, as can be observed in Figure 5. The effect of duty cycle and frequency on electrical discharge properties is very complex, resulting in a wide range of plasma parameters. In general, the increase of the duty cycle at the same frequency results in an increase of both the On stage and discharge durations, as shown in Figure 6.

The duration of glow discharge increases from approximately 100 μs for a 25% duty cycle (Figure 6a), to approximately 135 μs for a 30% duty cycle (Figure 6b), and to approximately 170 μs for a 35% duty cycle (Figure 6c) for the same PWM frequency of 1.5 kHz. Additionally, the increase of duty cycle results in a decrease of the Off stage duration, leading to an increase of the remaining charge stored in the reservoir capacitor after the Off stage and an insignificant decrease of the breakdown voltage. A change of duty cycle does not have a significant effect on the shape of the current and voltage waveforms, and only results in an increase of the duration of re-pulsing glow discharge. A change of glow discharge duration without a significant change of plasma properties could be used for the control of electric power dissipated in the plasma and a dose of plasma treatment.

On the other hand, the effect of frequency on glow discharge parameters is more complex. Figure 7 demonstrates the effect of PWM frequency on current and voltage waveforms when the duty cycle is fixed at 25%. The increase of frequency at the same duty cycle results in the decrease of the duration of both the On and Off stages, which affects discharge in a more complex way than simple duty-cycle variation. A frequency increase results in the decrease of

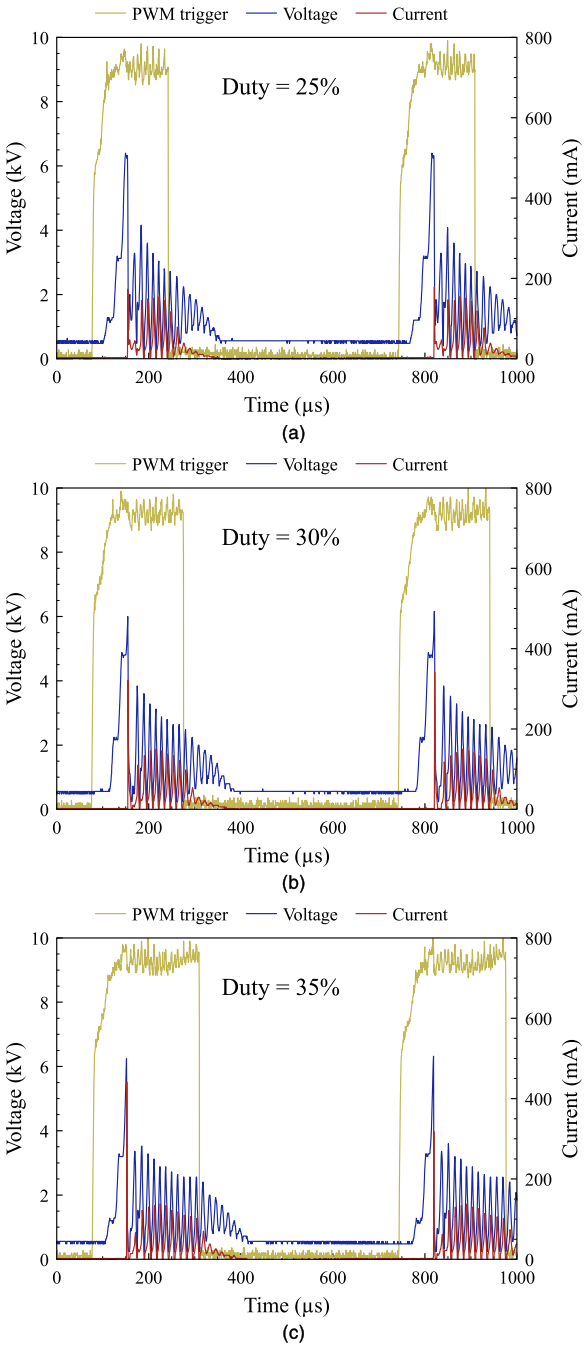

FIGURE 6. Current and voltage waveforms of re-pulsing glow discharges generated using PWM frequency of 1.5 kHz and PWM duty cycles of (a) 25%, (b) 30%, and (c) 35%.

re-pulsing glow discharge duration within a single PWM On stage: it decreases from approximately 415 μs for 0.5 kHz (Figure 7a), to approximately 100 μs for 1.5 kHz (Figure 7b), and to approximately 25 μs for 2.5 kHz (Figure 7c).

Interestingly, in the case of 2.5 kHz and 25% duty cycle, only one pulse of glow discharge is generated during the PWM On stage, followed by one more pulse of glow discharge after the end of the PWM On stage. It is possible to achieve single-pulse glow discharge followed by damping oscillation for higher frequencies; however, in this case,

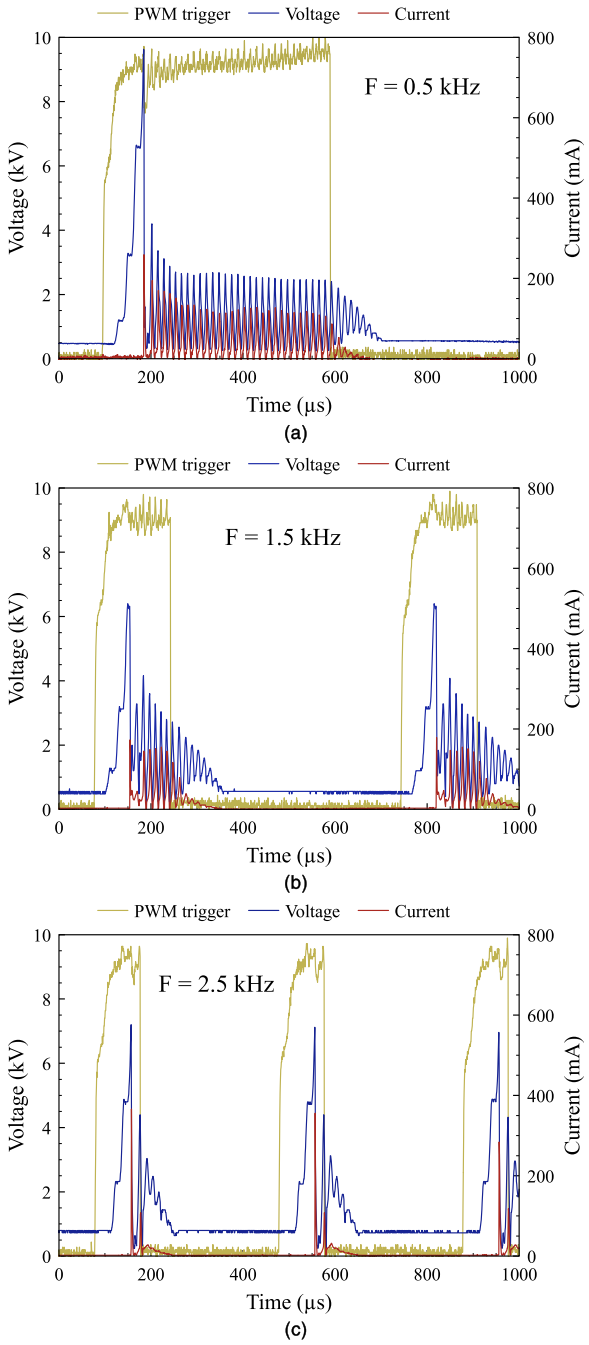

FIGURE 7. Current and voltage waveforms of re-pulsing glow discharges generated using PWM duty cycle of 25% and PWM frequencies of (a) 0.5 kHz, (b) 1.5 kHz, and (c) 2.5 kHz.

discharge would be highly unstable and continuously interrupted by sparks. Therefore, the upper frequency limit can be defined here as the one resulting in two-pulse discharge generation within a single PWM cycle.

On the other hand, the effect of frequency on breakdown voltage is more complex. With the increase of frequency from a low value (the lowest frequency value studied in this work was 0.5 kHz), the breakdown voltage decreases owing to a decrease of the Off stage duration and an increase of the charge remaining in the reservoir capacitor. However, at some point, the On stage decrease (induced by frequency growth) provokes a reduction of the charged particle density in the plasma afterglow, thus elevating the breakdown voltage. In the case of 25% duty cycle, the breakdown voltage decreases from approximately 10 kV for 0.5 kHz (Figure 7a) to 6.5 kV for 1.5 kHz (Figure 7b). At some point, it starts to increase with a further increase of frequency, reaching 7.2 kV for 2.5 kHz (Figure 7c).

By combining frequency and duty-cycle variation, one can control the dissipated energy in the glow discharge and the properties of the plasma itself. Figure 8 summarizes the values of electric power dissipated in the glow discharge (estimated by integration of current and voltage waveforms) as a function of the PWM frequency for various values of duty cycles.

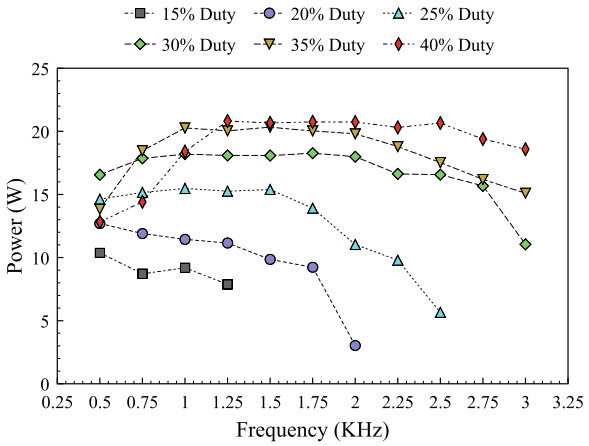

FIGURE 8. Electric power dissipated in re-pulsing glow discharge as a function of PWM frequency for various values of PWM duty cycles. All other parameters were kept constant in this series of measurements.

In Figure 8, each curve reflects the maximal range of frequencies available for each duty cycle value required to ensure the generation of stable re-pulsing glow discharge. For each duty cycle reported in Figure 8, there is a range of frequencies where the electric power dissipated in the glow discharge does not significantly change. Areas with lower or higher frequency values compared to the stable region corresponded to a lower power. The observed reduction in dissipated power could be explained by two effects. At frequencies lower than the optimal condition, the duration of the Off stage is long enough to cause an increase of the breakdown voltage, leading to the increase of time required for the charging of the reservoir capacitor to the required voltage. Since the overall On stage duration time is constant when the duty cycle is fixed, a frequency decrease results in an increase of charging time, and a decrease of overall (time-averaged) glow-discharge duration and power dissipated in the glow discharge. The same effect is observed with the increase of frequency. When frequency is above optimal condition an increase of breakdown voltage and a decrease in the discharge subpulse number, leading to extremely low energy consumption at the highest frequency allowed for a given duty cycle. On the other hand, in the

case of high frequencies, the duration of damping oscillation becomes comparable to a short On stage, resulting in the amount of energy consumed during the damping oscillation being comparable to energy dissipated in the plasma. A significant amount of energy consumed during damping oscillation without plasma leads to inefficient electric power use.

It can be concluded that the most important parameters for control of electric energy dissipated in plasma and plasma properties are the durations of On and Off stages, and the variation of PWM frequency and duty cycle is an effective way to control those parameters.

Another important advantage of using PWM is the capability to generate more stable glow discharge compared to the case of continuous re-pulsing glow discharge reported elsewhere [24]. In the case of a continuous re-pulsing glow discharge, the plasma may be easily distorted, elongated, or even terminated in the presence of surrounding gas flow. In the case when the gas flow is transverse to the plasma, elongation and restrike of the discharge occur in the same way as in the case of gliding glow discharge [49]. In the case when the gas flow is parallel to the plasma, the main source of elongation is the turbulence in the gas flow and plasma fluctuations. Therefore, for generation of a stable continuous glow discharge, it is required to use a sealed chamber without gas flow. Additionally, even inside a sealed chamber, a high plasma temperature may cause rather strong gas convection, thus compromising discharge uniformity (e.g., making the upper discharge area more intense compared to the lower area) and at certain conditions, resulting in discharge termination [24]. PWM pulsations, on the other hand, allow minimization of elongation due to the short duration of the discharge. If the frequency is high enough, discharge is always reignited at the place of the shortest gap between the electrodes, even in the presence of external airflow.

To study plasma properties in the presence of gas flow, the electrodes were placed in a quartz tube (14 mm inner diameter and 16 mm outer diameter), and gas was supplied from the bottom of the tube at a flow rate regulated by a mass-flow controller (Figure 5S, supplementary data).

Depending on the discharge parameters and gas-flow rate, pulse-width modulated glow discharge could be stable or slightly fluctuate inside the tube. For example, in the case of 2 slm airflow, the discharge is stable at 2.5 kHz (30% duty cycle), slightly fluctuates at 1.5 kHz (30% duty cycle), and the plasma is heavily distorted in the case of continuous discharge without PWM (Figure 6S, supplementary data). Fluctuation and elongation of the continuous glow discharge without PWM caused by gas flow, together with a restrike in the case of elongation above the critical value, are similar to gliding glow discharge systems. The main disadvantage of this type of discharge is the presence of plasma under various conditions, and constant changes of the plasma impedance. For gas conversion applications (nitrogen fixation, CO_2 conversion, etc.), a typically low- or moderate-temperature region (elongated glow discharge) of the gliding glow system is required to avoid excess heating of the treated gas, whereas the other part of the discharge with high temperature is not desired. As demonstrated in this work, by controlling the duty cycle and frequency along with the gas flow, it is possible to achieve stable or only slightly fluctuating glow discharges possessing a rather wide range of dissipated energy. This opens new possibilities for igniting and sustaining discharge with parameters required for effective gas conversion, avoiding discharge elongation and the presence of plasma with unwanted parameters. Additionally, a well-known reproducible waveform of current and voltage allows better load matching compared to typical gliding glow reactors with randomly changing impedance during plasma treatment. On the other hand, the ability to control electric power delivered to the generator using PWM adds more flexibility to the design of potential gas treatment systems for practical applications. In this way, several push-pull generators could be powered by a single DC PSU with control of the consumed power by PWM on each generator, which should reduce the cost also making plasma gas conversion more reliable comparing to other methods.

D. DIAGNOSTICS OF PULSE-WIDTH-MODULATED GLOW DISCHARGE

Numerous plasma parameters are responsible for effective gas conversion. The most important ones (such as the rotational and vibrational temperatures of the gas molecules, as well as the electron density) could be estimated from the optical emission spectra. Additionally, the appearance and intensity of certain emission lines demonstrate the production rate of different plasma species while the line intensity ratio could lead to the efficiency of gas conversion itself. Considering possible application in gas conversion systems, OES diagnostics of re-pulsing glow discharge were conducted, targeted at the investigation of the PWM effect on rotational and vibrational temperatures.

Figure 9 demonstrates the typical optical emission spectrum acquired in the glow discharge generated using a PWM duty cycle of 35%, frequency of 1.5 kHz, and airflow of 1 slm.

Prominent emission bands observed in the spectra are the N_2 second positive system (SPS) between 290 and 420 nm, OH emission bands at 307 and 309 nm, and NO^{γ} emission bands between 220 and 290 nm. Despite the strong emission of OH originating from the dissociation of water molecules present in air, no emission lines from the hydrogen Balmer series (H_α and H_β) are observed owing to the fast quenching of hydrogen excited states by gas molecules from the air.

Ambient-air glow discharge has been reported to be one of the most efficient for nitrogen fixation, which suggests that pulse-width modulated glow discharge could also be a promising candidate for efficient NO production. The strong (and dynamically changing as a result of varying discharge conditions) $NO\gamma$ ro-vibrational emission band found in our study is direct evidence of this statement.

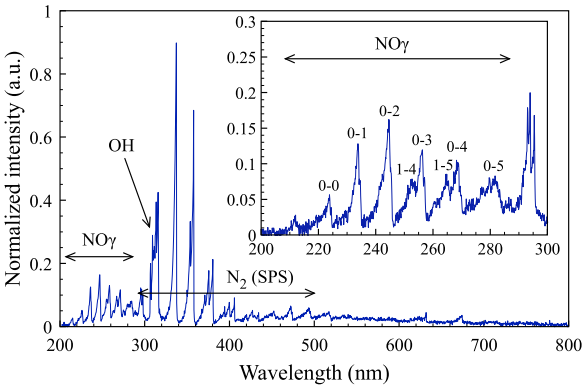

FIGURE 9. Typical optical emission spectrum of re-pulsing glow discharge with pulse-width modulation generated in ambient air recorded using 1200 grating. Spectral response of monochromator is not applied.

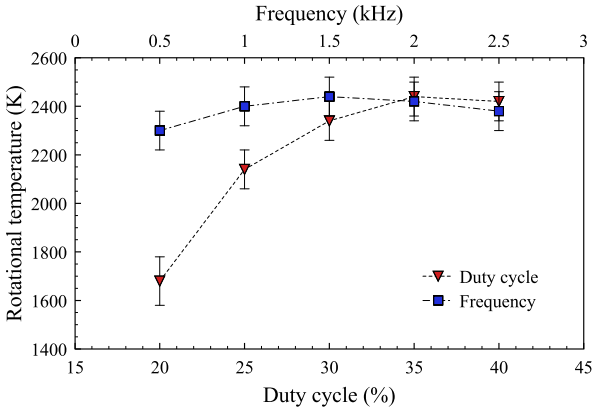

FIGURE 10. Rotational temperature as a function of PWM frequency for duty cycle of 30% and rotational temperature as a function of duty cycle for frequency of 1.5 kHz when the other parameters are fixed. The error bars correspond to the spectra fitting error.

The crucial parameters for effective gas conversion are the vibrational and rotational excitation of the molecules in the discharge. To demonstrate the possibility of the control of plasma parameters by pulse-width modulation in the presence of gas flow, discharges were generated with 0.5-2 slm airflow using varied PWM frequencies and duty cycles. Nitrogen emission bands were used for estimation of the time-averaged rotational and vibrational temperatures. Optical emission spectra were recorded using 500 accumulations, exposure time of 0.1 s, ICCD gate of 10 μs, and 4000 gate pulses per exposure leading to the emission intensity determination error of 2.96 %. The ICCD gate was not synchronized with the discharge resulting in the measurement of time-averaged spectra corresponding to the plasma ON time. As a measure of vibrational discharge excitation, the vibrational temperature of nitrogen in the $N_2(C)$ state was estimated due to its accessibility. Calculations were performed employing the N_2(C, delta v $= -3$) sequence using four detectable bandheads N_2(C, v' = 0-3); see supplementary data Figure 7S(a). Despite strong optical emission, N_2(C, delta v $= -2$) sequence was not used for calculation owing to appearance of only 3 detectable bandheads, leading to large error bars. The transition probabilities were taken from *Lofthus and Krupenie* [50]. Example of Boltzmann plot is presented on the Figure 7S(c), supplementary data. Vibrational temperature estimated for spectra measured within entire range of experimental parameters was around 4610 $\pm$ 770 K. After additional analysis, no clear trends in vibrational temperature were found depending on various discharge parameters (because of rather large experimental uncertainty).

Estimation of the rotational temperature of N_2 was done by comparison of the measured N_2 emission band at 380.5 nm to simulation data [24], [51]–[53]. An example of the measured and simulated spectrum is presented in Figure 8S (supplementary data). Rotational temperature as a function of frequency at a fixed duty cycle of 35% and airflow of 0.5 slm and vibrational temperature as a function of duty cycle at a fixed frequency of 1.5 kHz and airflow of 0.5 slm are presented in Figure 10. The frequency effect is rather minor, whereas rotational excitation clearly increases with the duty cycle and reaches saturation after 35% of duty. An increase in the rotational temperature from 1680 $\pm$ 100K to 2420 $\pm$ 90 K is clearly registered.

Analyzing the data presented in Figure 10 we should bear in mind that the average power remained nearly the same when the frequency changed, whereas it grew with the increase of the duty cycle, as mentioned above. The rather insignificant variation (given the apparent error bar values) of the rotational temperature is a reflection of electron-induced gas heating, where the energy transferred to the gas is defined by the average applied power and thus the total amount of electrons produced in the discharge volume (e-T transfer). Similarly, this is also valid for vibrational excitation (e-V transfer).

The observed increase and saturation of the rotational temperature with duty ratio clearly correspond to the change of the power dissipated in plasma as a result of duty cycle increase from 20 to 40% at a fixed frequency of 1.5 kHz (Figure 5). In this case gas may be heated more efficiently during longer pulses.

The found rotational temperature appears much lower than the vibrational one (mentioned above) clearly putting the studied discharge to the non-thermal type. The electron temperature was not measured in present work, which will be the subject for future studies.

Given the complexity of how the gas-flow rate, PWM duty cycle, and frequency alter the discharge parameters, it is difficult to study the effect of each variable parameter on the rotational temperature. Therefore, to determine the variation range of rotational temperature, which is possible to achieve by controlling the discharge conditions, a statistical approach (Taguchi method) was used [54], [55]. Experiments were planned using the Taguchi design, with the duty cycle varying in the range of 25% to 40% (25% was the minimal value for the generation of re-pulsing glow discharge at frequencies higher than 2 kHz at an airflow of 2 slm), frequency varying in the range of 1 to 2.5 kHz, and airflow varying in the range of 0.5 to 2 slm (Table IS and Figure 9S, supplementary data). The minimal rotational temperature of

approximately 1640 ± 100 K could be achieved at 25% duty, 2.5 kHz frequency, and 2 slm airflow, which were the marginal conditions featuring only two glow-discharge impulses during a PWM On stage. On the other hand, the maximal rotational temperature of 2440 ± 80 K is observed for a duty cycle of 35%, frequency of 1.5 kHz, and airflow of 0.5 slm. More details are given in Figure 9S (supplementary data). It could be concluded that the rotational temperature could be varied in the range of approximately 1640–2440 K by using only pulse-width modulation and the control of gas flow (the relative uncertainty of these values is approximately 10%).

As discussed above, a strong NO emission suggests the production of high-density NO, and together with discharge stabilization and control of rotational and vibrational temperatures by PWM even in the presence of external gas flow suggest that the pulse-width modulated re-pulsing glow discharge reported in this work could be used for energy-efficient nitrogen fixation. Additional control of the plasma parameters in the PWM case (as compared to the continuous case) could be beneficial for optimization of the gas conversion process, bringing the efficiency closer to theoretical limits and thus making plasma-based gas conversion more reliable compared to commonly used methods. However, for the practical use of re-pulsing glow discharge for nitrogen fixation, further analysis of the effect of the experiment conditions on NO production and energy required for the formation of NO molecules, together with the fine-tuning of these parameters, are desired. These studies are the subject of our future work.

In addition to the use in gas-conversion, the reported re-pulsing glow discharge could also be used in biomedical and agricultural applications. For example, by tuning gas flow and PWM parameters, it is possible to achieve a low temperature of the gas passing through the tube, which will make possible the exposure of biosamples to gas exhaust with a high concentration of long living reactive species. On the other hand, the discharge could be transferred to the surface of a liquid (including flowing liquid) in the same way as reported elsewhere for the production of plasma-activated liquids, which could be used in agriculture and medicine [23], [56]–[58].

IV. CONCLUSION

The possibility of generation of stable pulsed glow discharges operating in ambient air in a 2 cm gap was demonstrated. To achieve this goal, the pulse-width modulation concept was implemented, and a corresponding plasma generator was developed. As a result, a repeatable discharge containing multiple plasma pulses within a single On stage (the number of which is controllable) was obtained.

The obtained re-pulsing discharges revealed the properties of a glow discharge. However, the other types of discharges could also be generated in the case when the conditions were not suitable for the generation of re-pulsing glow. As a result, corona, diffuse corona, transient spark, spark-to-glow discharge sequence, and even glow discharge reignition without spark could be realized using the same power supply. Additionally, it was demonstrated that the type of discharge and total power dissipated in the plasma volume could be precisely controlled, and the discharge could be stabilized even in the presence of external airflow, taking the advantages of pulse-width modulation. Optical diagnostics of the discharge revealed that pulse-width modulation could also be used for the control of the plasma parameters. By variation of gas flow, PWM frequency and duty ratio, it was possible to control the electric power dissipated in the plasma in the range of 3-21 W, rotational temperature of molecular nitrogen in the range of 1640-2440 K, and its vibrational temperature around 4610 K.

The generation of stable glow discharge in the presence of gas flow with additional control of plasma properties by pulse-width modulation looks promising for use in energy-efficient gas conversion.

Further analysis of NO production and fine-tuning of the experiment conditions are required for practical use in nitrogen fixation and other applications in gas conversion.

REFERENCES

[1] N. Saito, M. A. Bratescu, and K. Hashimi, "Solution plasma: A new reaction field for nanomaterials synthesis," *Jpn. J. Appl. Phys.*, vol. 57, no. 1, 2018, Art. no. 0102A4.

[2] J. Winter, R. Brandenburg, and K.-D. Weltmann, "Atmospheric pressure plasma jets: An overview of devices and new directions," *Plasma Sources Sci. Technol.*, vol. 24, no. 6, Oct. 2015, Art. no. 064001.

[3] S. Bekeschus, A. Schmidt, K.-D. Weltmann, and T. von Woedtke, "The plasma jet kINPen—A powerful tool for wound healing," *Clin. Plasma Med.*, vol. 4, no. 1, pp. 19–28, Jul. 2016.

[4] P. Bruggeman *et al.*, "Plasma-liquid interactions: A review and roadmap," *Plasma Sources Sci. Technol.*, vol. 25, no. 5, Sep. 2016, Art. no. 053002.

[5] E. Y. Gusev, O. A. Ageev, V. A. Gamaleev, A. S. Mikhno, O. O. Mironenko, and E. A. Pronin, "Effect of annealing on conductivity type of nanocrystalline ZnO films fabricated by RF magnetron sputtering," *Adv. Mater. Res.*, vol. 893, pp. 539–542, Feb. 2014.

[6] M. Ito, J.-S. Oh, T. Ohta, M. Shiratani, and M. Hori, "Current status and future prospects of agricultural applications using atmospheric-pressure plasma technologies," *Plasma Processes Polym.*, vol. 15, no. 2, Feb. 2018, Art. no. 1700073.

[7] J. Zhang, T. Kwon, S. Kim, and D. Jeong, "Plasma farming: Non-thermal dielectric barrier discharge plasma technology for improving the growth of soybean sprouts and chickens," *Plasma*, vol. 1, no. 2, pp. 285–296, Dec. 2018.

[8] N. Puač, M. Gherardi, and M. Shiratani, "Plasma agriculture: A rapidly emerging field," *Plasma Processes Polym.*, vol. 15, no. 2, Feb. 2018, Art. no. 1700174.

[9] I. Schweigert, D. Zakrevsky, P. Gugin, E. Yelak, E. Golubitskaya, O. Troitskaya, and O. Koval, "Interaction of cold atmospheric argon and helium plasma jets with bio-target with grounded substrate beneath," *Appl. Sci.*, vol. 9, no. 21, p. 4528, Oct. 2019.

[10] S. Ito, K. Sakai, V. Gamaleev, M. Ito, M. Hori, M. Kato, and M. Shimizu, "Oxygen radical based on non-thermal atmospheric pressure plasma alleviates lignin-derived phenolic toxicity in yeast," *Biotechnol. Biofuels*, vol. 13, no. 1, p. 18, Dec. 2020.

[11] H. Tanaka, M. Mizuno, K. Ishikawa, S. Toyokuni, H. Kajiyama, F. Kikkawa, and M. Hori, "New hopes for plasma-based cancer treatment," *Plasma*, vol. 1, no. 1, pp. 150–155, Aug. 2018.

[12] Y. Sato, S. Yamada, S. Takeda, N. Hattori, K. Nakamura, H. Tanaka, M. Mizuno, M. Hori, and Y. Kodera, "Effect of plasma-activated lactated Ringer's solution on pancreatic cancer cells *in vitro* and *in vivo*," *Ann. Surgical Oncol.*, vol. 25, no. 1, pp. 299–307, Jan. 2018.

[13] H. Tanaka, M. Mizuno, Y. Katsumata, K. Ishikawa, H. Kondo, H. Hashizume, Y. Okazaki, S. Toyokuni, K. Nakamura, N. Yoshikawa, H. Kajiyama, F. Kikkawa, and M. Hori, "Oxidative stress-dependent and -independent death of glioblastoma cells induced by non-thermal plasma-exposed solutions," *Sci. Rep.*, vol. 9, no. 1, p. 13657, Dec. 2019.

[14] H. Tanaka, K. Nakamura, M. Mizuno, K. Ishikawa, K. Takeda, H. Kajiyama, F. Utsumi, F. Kikkawa, and M. Hori, "Non-thermal atmospheric pressure plasma activates lactate in Ringer's solution for anti-tumor effects," *Sci. Rep.*, vol. 6, no. 1, p. 36282, Dec. 2016.

[15] W. Wang, B. Patil, S. Heijkers, V. Hessel, and A. Bogaerts, "Nitrogen fixation by gliding arc plasma: Better insight by chemical kinetics modelling," *ChemSusChem*, vol. 10, no. 10, pp. 2145–2157, May 2017.

[16] B. S. Patil, Q. Wang, V. Hessel, and J. Lang, "Plasma N2-fixation: 1900–2014," *Catal. Today*, vol. 256, pp. 49–66, Nov. 2015.

[17] B. S. Patil, F. J. J. Peeters, G. J. van Rooij, J. A. Medrano, F. Gallucci, J. Lang, Q. Wang, and V. Hessel, "Plasma assisted nitrogen oxide production from air: Using pulsed powered gliding arc reactor for a containerized plant," *AIChE J.*, vol. 64, no. 2, pp. 526–537, Feb. 2018.

[18] X. Hao, A. M. Mattson, C. M. Edelblute, M. A. Malik, L. C. Heller, and J. F. Kolb, "Nitric oxide generation with an air operated non-thermal plasma jet and associated microbial inactivation mechanisms," *Plasma Processes Polym.*, vol. 11, no. 11, pp. 1044–1056, Nov. 2014.

[19] X. L. Deng, A. Y. Nikiforov, P. Vanraes, and C. Leys, "Direct current plasma jet at atmospheric pressure operating in nitrogen and air," *J. Appl. Phys.*, vol. 113, no. 2, Jan. 2013, Art. no. 023305.

[20] J. Yang, T. Li, C. Zhong, X. Guan, and C. Hu, "Nitrogen fixation in water using air phase gliding arc plasma," *J. Electrochem. Soc.*, vol. 163, no. 10, pp. E288–E292, 2016.

[21] X. Pei, D. Gidon, Y.-J. Yang, Z. Xiong, and D. B. Graves, "Reducing energy cost of NO production in air plasmas," *Chem. Eng. J.*, vol. 362, pp. 217–228, Apr. 2019.

[22] Y. D. Korolev, O. B. Frants, N. V. Landl, A. V. Bolotov, and V. O. Nekhoroshev, "Features of a near-cathode region in a gliding arc discharge in air flow," *Plasma Sources Sci. Technol.*, vol. 23, no. 5, Sep. 2014, Art. no. 054016.

[23] V. Gamaleev, N. Iwata, G. Ito, M. Hori, M. Hiramatsu, and M. Ito, "Scalable treatment of flowing organic liquids using ambient-air glow discharge for agricultural applications," *Appl. Sci.*, vol. 10, no. 3, p. 801, Jan. 2020.

[24] V. Gamaleev, T. Tsutsumi, M. Hiramatsu, M. Ito, and M. Hori, "Generation and diagnostics of ambient air glow discharge in centimeter-order gaps," *IEEE Access*, vol. 8, pp. 72607–72619, 2020.

[25] W. P. Allis, "Review of glow discharge instabilities," *Phys. B+C*, vol. 82, no. 1, pp. 43–51, Mar. 1976.

[26] J. T. Gudmundsson and A. Hecimovic, "Foundations of DC plasma sources," *Plasma Sources Sci. Technol.*, vol. 26, no. 12, Nov. 2017, Art. no. 123001.

[27] M. R. Winchester and R. Payling, "Radio-frequency glow discharge spectrometry: A critical review," *Spectrochim. Acta B, At. Spectrosc.*, vol. 59, pp. 607–666, 2004.

[28] Y. P. Raizer, *Gas Discharge Physics*, 1st ed. Berlin, Germany: Springer-Verlag, 1991.

[29] A.-A.-H. Mohamed, R. Block, and K. H. Schoenbach, "Direct current glow discharges in atmospheric air," *IEEE Trans. Plasma Sci.*, vol. 30, no. 1, pp. 182–183, Feb. 2002.

[30] P. Bruggeman, J. Liu, J. Degroote, M. G. Kong, J. Vierendeels, and C. Leys, "DC excited glow discharges in atmospheric pressure air in pin-to-water electrode systems," *J. Phys. D, Appl. Phys.*, vol. 41, no. 21, Nov. 2008, Art. no. 215201.

[31] D. Staack, B. Farouk, A. Gutsol, and A. Fridman, "Characterization of a DC atmospheric pressure normal glow discharge," *Plasma Sources Sci. Technol.*, vol. 14, no. 4, pp. 700–711, Nov. 2005.

[32] D. Staack, B. Farouk, A. F. Gutsol, and A. A. Fridman, "Spectroscopic studies and rotational and vibrational temperature measurements of atmospheric pressure normal glow plasma discharges in air," *Plasma Sources Sci. Technol.*, vol. 15, no. 4, pp. 818–827, Nov. 2006.

[33] X. Li, P. Zhang, P. Jia, J. Chu, and J. Chen, "Generation of a planar direct-current glow discharge in atmospheric pressure air using rod array electrode," *Sci. Rep.*, vol. 7, no. 1, p. 2672, Dec. 2017.

[34] V. I. Arkhipenko, A. A. Kirillov, Y. A. Safronau, and L. V. Simonchik, "DC atmospheric pressure glow microdischarges in the current range from microamps up to amperes," *Eur. Phys. J. D*, vol. 60, no. 3, pp. 455–463, Dec. 2010.

[35] M. L. Williams, *CRC Handbook of Chemistry and Physics*, 84th ed. Boca Raton, FL, USA: CRC Press, 2004.

[36] W. T. Shugg, *Handbook of Electrical and Electronic Insulating Materials*. New York, NY, USA: Van Nostrand Reinhold, 1986.

[37] D. Staack, B. Farouk, A. Gutsol, and A. Fridman, "DC normal glow discharges in atmospheric pressure atomic and molecular gases," *Plasma Sources Sci. Technol.*, vol. 17, no. 2, May 2008, Art. no. 025013.

[38] O. Mutaf-yardimci, A. V. Saveliev, A. A. Fridman, and L. A. Kennedy, "Thermal and nonthermal regimes of gliding arc discharge in air flow," *J. Appl. Phys.*, vol. 87, no. 4, p. 1632, Jan. 2000.

[39] J. Pawłat, P. Terebun, M. Kwiatkowski, B. Tarabová, Z. Kovalová, K. Kučerová, Z. Machala, M. Janda, and K. Hensel, "Evaluation of oxidative species in gaseous and liquid phase generated by mini-gliding arc discharge," *Plasma Chem. Plasma Process.*, vol. 39, no. 3, pp. 627–642, May 2019.

[40] S. Gröger, M. Ramakers, M. Hamme, J. A. Medrano, N. Bibinov, F. Gallucci, A. Bogaerts, and P. Awakowicz, "Characterization of a nitrogen gliding arc plasmatron using optical emission spectroscopy and high-speed camera," *J. Phys. D, Appl. Phys.*, vol. 52, no. 6, Feb. 2019, Art. no. 065201.

[41] H. Zhang, L. Li, X. Li, W. Wang, J. Yan, and X. Tu, "Warm plasma activation of CO_2 in a rotating gliding arc discharge reactor," *J. CO_2 Utilization*, vol. 27, pp. 472–479, Oct. 2018.

[42] Y. D. Korolev, O. B. Frants, N. V. Landl, and A. I. Suslov, "Low-current plasmatron as a source of nitrogen oxide molecules," *IEEE Trans. Plasma Sci.*, vol. 40, no. 11, pp. 2837–2842, Nov. 2012.

[43] S. Li, J. Medrano Jimenez, V. Hessel, and F. Gallucci, "Recent progress of plasma-assisted nitrogen fixation research: A review," *Processes*, vol. 6, no. 12, p. 248, Dec. 2018.

[44] V. F. Tarasenko, E. K. Baksht, I. D. Kostyrya, and V. Shutko, "Runaway electron preionized diffuse discharges in atmospheric pressure air with a point-to-plane gap in repetitive pulsed mode," *J. Appl. Phys.*, vol. 109, no. 8, Apr. 2011, Art. no. 083306.

[45] Z. Machala, I. Jedlovsky, and V. Martisovits, "DC discharges in atmospheric air and their transitions," *IEEE Trans. Plasma Sci.*, vol. 36, no. 4, pp. 918–919, Aug. 2008.

[46] Y. Akishev, M. Grushin, I. Kochetov, V. Karal'nik, A. Napartovich, and N. Trushkin, "Negative corona, glow and spark discharges in ambient air and transitions between them," *Plasma Sources Sci. Technol.*, vol. 14, no. 2, pp. S18–S25, May 2005.

[47] Y. Akishev, M. Grushin, V. Karalnik, A. Petryakov, and N. Trushkin, "Non-equilibrium constricted DC glow discharge in N2flow at atmospheric pressure: Stable and unstable regimes," *J. Phys. D, Appl. Phys.*, vol. 43, no. 7, Feb. 2010, Art. no. 075202.

[48] C. Kong, J. Gao, J. Zhu, A. Ehn, M. Aldén, and Z. Li, "Re-igniting the afterglow plasma column of an AC powered gliding arc discharge in atmospheric-pressure air," *Appl. Phys. Lett.*, vol. 112, no. 26, Jun. 2018, Art. no. 264101.

[49] A. Fridman, S. Nester, L. A. Kennedy, A. Saveliev, and O. Mutaf-Yardimci, "Gliding arc gas discharge," *Prog. Energy Combustion Sci.*, vol. 25, no. 2, pp. 211–231, Apr. 1999.

[50] A. Lofthus and P. H. Krupenie, "The spectrum of molecular nitrogen," *J. Phys. Chem. Ref. Data*, vol. 6, pp. 113–307, Jan. 1977.

[51] T.-L. Zhao, Y. Xu, Y.-H. Song, X.-S. Li, J.-L. Liu, J.-B. Liu, and A.-M. Zhu, "Determination of vibrational and rotational temperatures in a gliding arc discharge by using overlapped molecular emission spectra," *J. Phys. D, Appl. Phys.*, vol. 46, no. 34, Aug. 2013, Art. no. 345201.

[52] N. Britun, M. Gaillard, S.-G. Oh, and J. G. Han, "Fabry–Perot interferometry for magnetron plasma temperature diagnostics," *J. Phys. D, Appl. Phys.*, vol. 40, no. 17, pp. 5098–5108, Sep. 2007.

[53] P. J. Bruggeman, N. Sadeghi, D. C. Schram, and V. Linss, "Gas temperature determination from rotational lines in non-equilibrium plasmas: A review," *Plasma Sources Sci. Technol.*, vol. 23, no. 2, Apr. 2014, Art. no. 023001.

[54] A. Pander, A. Hatta, and H. Furuta, "Optimization of catalyst formation conditions for synthesis of carbon nanotubes using taguchi method," *Appl. Surf. Sci.*, vol. 371, pp. 425–435, May 2016.

[55] V. Gamaleev, N. Iwata, M. Hiramatsu, and M. Ito, "Tuning of operational parameters for effective production of nitric oxide using an ambient air rotating glow discharge jet," *Jpn. J. Appl. Phys.*, vol. 59, no. SH, May 2020, Art. no. SHHF04.
[56] V. Gamaleev, N. Iwata, M. Hori, M. Hiramatsu, and M. Ito, "Direct treatment of liquids using low-current arc in ambient air for biomedical applications," *Appl. Sci.*, vol. 9, no. 17, p. 3505, Aug. 2019.
[57] M. Schmidt, V. Hahn, B. Altrock, T. Gerling, I. C. Gerber, K.-D. Weltmann, and T. von Woedtke, "Plasma-activation of larger liquid volumes by an inductively-limited discharge for antimicrobial purposes," *Appl. Sci.*, vol. 9, no. 10, p. 2150, May 2019.
[58] N. Iwata, V. Gamaleev, H. Hashizume, J. Oh, T. Ohta, K. Ishikawa, M. Hori, and M. Ito, "Simultaneous achievement of antimicrobial property and plant growth promotion using plasma-activated benzoic compound solution," *Plasma Processes Polym.*, vol. 16, no. 8, Aug. 2019, Art. no. 1900023.

VLADISLAV GAMALEEV (Member, IEEE) received the M.Sc. degree from Southern Federal University, Russia, in 2011, and the Dr.Eng. degree from the Kochi University of Technology, Japan, in 2018. He is currently a Postdoctoral Researcher with Nagoya University, Nagoya, Japan. His research interests include plasma generation at atmospheric and high pressure in gas and liquid phase and plasma diagnostics. He is also focusing on biomedical and agricultural applications of atmospheric pressure plasmas. He is a member of the Japan Society of Applied Physics (JSAP).

NIKOLAY BRITUN graduated from the Radiophysical Department (Quantum Radiophysics Division), Kiev National University, Ukraine. He received the Ph.D. degree in plasma diagnostics from Sungkyunkwan University, South Korea, in 2008. From 2009 to 2019, he was with the Laboratory of Chimie des Interactions Plasma-Surface (Chemistry of Plasma-Surface Interactions), University of Mons, Belgium, first as a Postdoctoral researcher, and later as a Senior Researcher dealing mainly with magnetron sputtering, atmospheric, and microwave discharge diagnostics. He is currently an Associate Professor with Nagoya University, Japan. His main interests include plasma spectroscopy, including laser diagnostics and covering various low-pressure and atmospheric discharges.

MASARU HORI (Member, IEEE) received the B.E. and M.E. degrees from Waseda University, Tokyo, Japan, in 1981 and 1983, respectively, and the D.E. degree from Nagoya University, Nagoya, Japan, in 1986. He was a Researcher with Toshiba Corporation from 1986 to 1992. He was a Research Associate, an Assistant Professor, and then an Associate Professor with Nagoya University, from 1992 to 2004, where he has been a Professor, since 2004. He was the Director of the Plasma Nano Research Center, from 2009 to 2013. He was the Director of Plasma Medical Science Global Innovation Center, Nagoya University, from 2013 to 2019, where he has also been the Director of Center for Low-temperature Plasma Science, since 2019. His current research interests include plasma nano-processing and life sciences.